

# MSP : Refine Boundary Segmentation via Multiscale Superpixel

Jie Zhu<sup>1</sup>, Huabin Huang<sup>2</sup>, Banghuai Li<sup>2</sup>, Yong Liu<sup>3</sup>, Leye Wang<sup>1\*</sup>

<sup>1</sup>Peking University <sup>2</sup>Megvii Inc <sup>3</sup>Beihang University  
 zhujie@stu.pku.edu.cn, {huanghuabin, libanghuai}@megvii.com,  
 yongliu@buaa.edu.cn, leyewang@pku.edu.cn

## Abstract

In this paper, we propose a simple but effective message passing method to improve the boundary quality for the semantic segmentation result. Inspired by the generated sharp edges of superpixel blocks, we employ superpixel to guide the information passing within feature map. Simultaneously, the sharp boundaries of the blocks also restrict the message passing scope. Specifically, we average features that the superpixel block covers within feature map, and add the result back to each feature vector. Further, to obtain sharper edges and farther spatial dependence, we develop a multiscale superpixel module (MSP) by a cascade of different scales superpixel blocks. Our method can be served as a plug-and-play module and easily inserted into any segmentation network without introducing new parameters. Extensive experiments are conducted on three strong baselines, namely PSPNet, DeeplabV3, and DeepLabV3+, and four challenging scene parsing datasets including ADE20K, Cityscapes, PASCAL VOC, and PASCAL Context. The experimental results verify its effectiveness and generalizability.

## Introduction

Semantic segmentation is a fundamental and challenging problem of computer vision, whose goal is to assign a semantic category to each pixel of the image. It is critical for various tasks such as autonomous driving, image editing, and robot sensing. Recently, with the rapid development of deep learning, fully convolutional (Long, Shelhamer, and Darrell 2015) based methods have been proposed to address the above task. These methods have achieved significant performance on various benchmarks (Zhou et al. 2017; Cordts et al. 2016; Everingham et al. 2015; Mottaghi et al. 2014). However, many researchers have also noticed that segmented boundary is of low quality to some extent. Therefore, many efforts are devoted to improving the performance of boundary segmentation. DenseCRF (Krähenbühl and Koltun 2012), as a classic method, uses color and position relationship of the original pixels of the image to refine the segmentation results containing poor boundary (Chen et al. 2014, 2017a; Zheng et al. 2015). However, DenseCRF usually serves as a post-processing module, which makes it not closely integrated

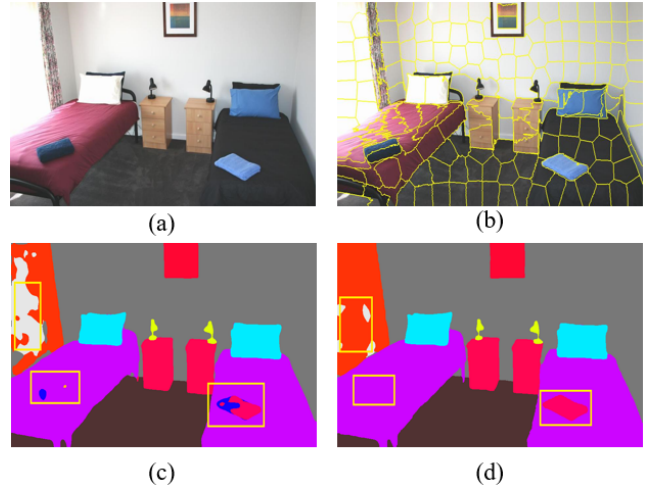


Figure 1: (a): An image from ADE20K datasets (b): Superpixel that aggregates similar pixels and groups them into blocks of different sizes and shapes according to low-level features such as the color, texture, and pixel location of the image. (c): Segmentation output from DeepLabV3+. (d): Refined segmentation by our method.

with the CNN structure, and has a weak effect on optimizing the feature representation of edge points. Afterward, some works (Wang et al. 2018a; Huang et al. 2019) leverage attention mechanism of the high-level features to construct more reliable context information between the edge points and the internal points of the object. Some other works (Bertasius, Shi, and Torresani 2016; Takikawa et al. 2019; Yuan et al. 2020) exploit as much boundary information as possible via deep neural networks. For example, SegFix (Yuan et al. 2020) encodes the relative distance information of the boundary pixels with a boundary map and a direction map, correcting the wrongly classified boundary pixels via internal points with high confidence. However, the accuracy of the weights or relationships obtained by these methods closely depends on the purity of the high-level features, which is what the edge feature points lack. The boundary features usually contain multiple object information due to the large receptive field of CNN. Therefore, the performance improvement brought by

\*corresponding author

these methods is limited.

Superpixels are an over-segmentation of an image that is formed by grouping image pixels based on the basic characteristics of the image, such as color, texture, and pixel position relationship. They provide a perceptually meaningful tessellation of image content, thereby reducing the number of image primitives. Due to their representational and computational efficiency, superpixels have turned into an accepted low/mid-level image representation. Many previous works (Shu, Dehghan, and Shah 2013; Yan et al. 2015; Zhu et al. 2014) have employed this advantage and acquired pretty results. On the other hand, the generated pixel blocks usually contain sharp edges as shown in Fig. 1 (b), which is also worth exploring for downstream tasks like semantic segmentation.

Thus, in this paper, we propose a simple but effective superpixel guided message passing method to correct wrongly segmented boundaries with the help of its sharp boundary. Further, inspired by the multiscale image pyramid, we design a multiscale superpixel information passing module (MSP), enabling multiple sharper edges and farther spatial dependence by a cascade of different scales superpixel blocks. These multiscale superpixel blocks are utilized to replace the high-level features to guide message passing within feature map. Simultaneously, the sharp boundaries of the blocks also restrict the message passing scope, making neighboring boundary features acquire messages from different block sides. Finally, extensive evaluations of our multiscale superpixel algorithm on ADE20K, Cityscapes, PASCAL VOC, and PASCAL Context datasets are conducted to demonstrate its effectiveness and generalizability. A pair of segmentation visualization contrast can be found in Fig. 1 (c) and (d). The main contributions of this work are summarized as follows:

- We propose a simple but useful algorithm to refine semantic segmentation boundaries by superpixel because of its sharp edges and local consistency in a large area.
- A multiscale superpixel module is designed to obtain sharper edges and farther spatial dependence.
- Our method has obtained general improvement in semantic segmentation on three outstanding networks and four widely used scene parsing datasets.

## Related Works

**Semantic Segmentation.** Driven by powerful deep neural networks (Krizhevsky, Sutskever, and Hinton 2012; Simonyan and Zisserman 2014; Szegedy et al. 2015), pixel-level prediction tasks like scene parsing and semantic segmentation achieve great progress inspired by replacing the fully-connected layer in classification with the convolution layer (Long, Shelhamer, and Darrell 2015). To enlarge the receptive field of neural networks, several model variants are proposed. For example, GCN (Peng et al. 2017) adopts decoupling of large kernel convolution to gain a large receptive field for the feature map and capture long-range information. DeeplabV3 (Chen et al. 2017b) extends ASPP with image-level feature to further capture global contexts. DeeplabV3+ (Chen et al. 2018) adds a decoder upon DeeplabV3 to refine the segmentation results, especially along object boundaries. The success of self-attention mechanism in natural language processing attracts lots of researchers’ attention.

DANet(Fu et al. 2019) applies both spatial and channel attention to gather information around the feature maps, which costs even more computation and memory than the Nonlocal(Wang et al. 2018b) method. EMANet(Li et al. 2019) integrates Expectation-Maximization (EM) algorithm to CNN to estimate attention map and reconstruct feature map while saving computing resources.

**Superpixel.** Superpixel is pixels with similar characteristics that are grouped together to form a larger block. Since its introduction in 2003 (Ren and Malik 2003), there have been many pretty excellent algorithms(Achanta et al. 2012; Weikersdorfer, Schick, and Cremers 2013; Van den Bergh et al. 2012) and mature evaluation metrics such as Undersegmentation Error. Moreover, publicly available superpixel algorithms have turned into standard tools in low-level vision. (Stutz, Hermans, and Leibe 2018) conducts fair analysis and evaluation of 28 superpixel algorithms on 5 datasets. Recently, in (Jampani et al. 2018), neural network is applied to the generation of superpixel and great results are achieved. Superpixels have been applied in target detection (Shu, Dehghan, and Shah 2013; Yan et al. 2015), semantic segmentation (Gould et al. 2008; Sharma, Tuzel, and Liu 2014; Gadde et al. 2016), saliency estimation (He et al. 2015; Perazzi et al. 2012; Yang et al. 2013; Zhu et al. 2014). (Yan et al. 2015) converts object detection problem into superpixel labeling problem and conducts an energy function considering appearance, spatial context and numbers of labels. (Gadde et al. 2016) uses superpixels to change how information is stored in the higher level of a CNN. In (He et al. 2015), superpixels are taken as input and contextual information is recovered among superpixels, which enables large context to be involved in the analysis efficiently.

**Refinement for Segmentation.** Previous work (Zheng et al. 2015; Lin et al. 2017a; Chen et al. 2017a) improved their segmentation results by DenseCRF (Krähenbühl and Koltun 2012). However, the low confidence score of the unary potential in boundary leads to a weak improvement of the object boundary segmentation, even with the help of pairwise potential. Recent works (Acuna, Kar, and Fidler 2019; Chen et al. 2019) extended the conventional level-set scheme to deep network for regularizing the boundaries of predicted segmentation map. Other studies (Bertasius, Shi, and Torresani 2016; Ding et al. 2019; Ke et al. 2018; Takikawa et al. 2019; Yuan et al. 2020) also exploit the boundary information to improve the segmentation. These works aim at correct classification of edge pixels, by utilizing high-level features to directly or indirectly guide message passing for reliable boundary feature representations. For example, SegFix (Yuan et al. 2020) encodes the relative distance information of the boundary pixels with a boundary map and a direction map to correct the wrong boundary pixels.

In this paper, we propose to refine segmentation via using superpixel blocks to guide the passing of information between features. Further, we design a plug-and-play multiscale superpixel module named MSP for sharper edges and longer dependency. Our method has been embedded in three famous semantic segmentation networks and evaluated on four challenging datasets. General gains brought by our method show its great potential.

## Approach

In this section, we present our simple but effective method named multiscale superpixel module (MSP). Before that, we firstly give a detailed description of our single scale superpixel guided message passing model (SSP). Afterward, we introduce the multiscale superpixel model. Finally, we give an example of a combination with DeeplabV3+ (Chen et al. 2018) that is considered as our baseline in most experiments and analyze the advantages of our proposed method.

### Superpixel Guided Message Passing

We use the superpixel segmentation algorithm to divide an image into hundreds of pixel blocks. These blocks define their respective scope of message passing. The  $i$ -th pixel block is denoted as  $p_i$ . In an image, all generated pixel blocks belong to the set  $P$ .  $K$  is the total number of elements in the set  $P$ . The entire information passing process consists of two steps: 1) computing averaged feature inside a superpixel; 2) adding it back to each pixel feature. Here, superpixel plays a role of a mask. More specifically, for the  $i$ -th superpixel block  $p_i$ , our approach averages the features inside the  $p_i$  superpixel and adds the mean value  $\bar{x}_i$  back to each feature vector covered by superpixel  $p_i$ . In order to obtain the mean feature map  $\bar{X}$  of the entire feature map  $X$ , it is necessary to enumerate all pixel blocks from 1 to  $K$ . Finally,  $\bar{X}$  is weighted to the original  $X$  to realize the message passing. The whole algorithm can also be formulated by the following formula:

$$\bar{X} = \sum_{i=1}^K \frac{S(P_i, X)}{N(P_i)}, \quad (1)$$

$$S(P_i, X) = \sum P_i \times X, \quad (2)$$

and

$$X^* = X + \alpha \bar{X}. \quad (3)$$

$P_i$  is a binary map with the same size as  $X$ , and the value in the  $p_i$  pixel block area is set to 1 (otherwise 0). The function  $S(\cdot)$  sums feature value in  $X$  along spacial dimension where the location is provided by  $P_i$ . The function  $N(\cdot)$  calculates the area of the  $p_i$  pixel block.  $\alpha$  is the weighting coefficient that is set to 0.1 by default.

Thus, superpixel blocks, as low-level features, successfully guide the fusion of high-level information. This method is not only simple but also effective for the improvement of the boundary because the superpixel blocks with sharp boundaries allow adjacent edges from two or more objects to receive the information from respective inside pixel blocks. This greatly boosts the discrimination of boundary features, especially for objects with obvious differences in characteristics.

In order to utilize the information of more features in a pixel block and avoid the excessive influence of a single feature vector, we average the features inside a pixel block and add it back to the original features with appropriate weight. In this way, each vector on the original feature map acquires the mean feature information within the pixel block where the vector is located. Note that this method introduces no convolution structure but still guarantees the backpropagation. The entire message passing process is presented in Fig. 2.

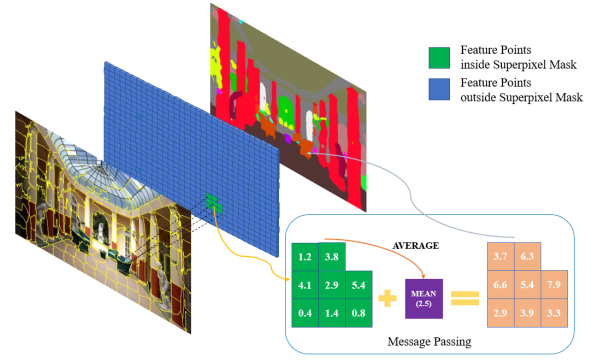


Figure 2: Superpixel Guided Message Passing. A superpixel block is first mapped to a corresponding area in the feature map, and then the averaged feature in that area is regarded as a passing message and added back to the area.

In the experimental part, this method has achieved good results beyond the baseline, which proves its effectiveness.

### Multiscale Superpixel Module

We consider that the single scale superpixel module (SSP) may lack diversity. And multiscale manner used to be a general solution that provides more details and broader context information. Therefore, we refer to the multiscale pyramid model and accordingly construct a multiscale superpixel model (MSP) in the process of information fusion. However, the key point where the model we design changes is not the size of the image but the number  $\lambda$  of superpixel blocks in an image that is divided. It is obvious that the shape of superpixel is irregular, which cannot be standardized and uniformly described. For the convenience of description, we define  $\lambda$  as the scale of superpixels. It is worth noticing that the larger the  $\lambda$  is, the greater the number of superpixel blocks in an image is, and the smaller the area of each pixel block is. In other words, a pixel block in an image may have a certain overlap with several pixel blocks on the other superpixel scales of that image, or it may be a part of a pixel block on another smaller scale as shown in Fig. 3. As a result, the multiscale model makes a wider range of cross-fusion of features available.

In terms of the specific implementation, the multiscale model is formed by cascade single scale models. This makes the information passing of every single scale independent from each other, thereby avoiding the problem of message confusion between multiple scales in a parallel fashion. In practice, the cascade fashion is easy to implement. Moreover, when cascade, the order of superpixel scale is from a small scale to a large scale, such as 100, 200, and 300. In other words, we first conduct the message passing in a large superpixel area, then followed by a smaller one. Such a sequence guarantees that information holds longer dependence as small scale superpxiel often has a certain overlap with large scale.

In order to present our multiscale model more clearly and intuitively, we attempt to use a simple formula to illustrate it. Firstly, we define the single scale model as the function  $F(X, \lambda, I)$ , and  $X^*$  is its output. So we can obtain the fol-

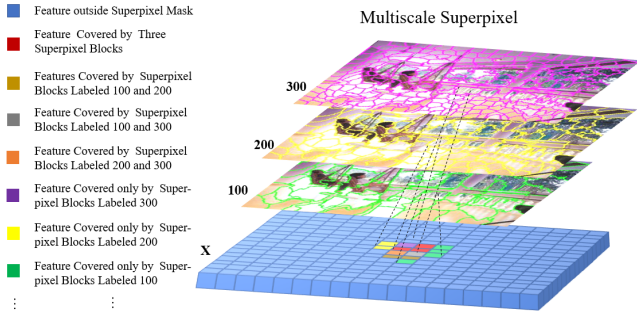


Figure 3: Illustration on multiscale superpixel overlap. Due to different sizes of pixel blocks between different scales, some areas between pixel blocks of different scales may contain overlap to some extent.

lowing formula:

$$X^* = F(X, \lambda, I), \quad (4)$$

where  $X$  is the original input feature,  $\lambda$  (superpixel scale) is the number of superpixel blocks in a picture, and  $I$  is a raw RGB image that is utilized to generate superpixel.

Then we present the formulas for a multiscale model based on the cascade of single scale models:

$$X_0^* = F(X, \lambda_0, I), \quad (5)$$

$$X_1^* = F(X_0^*, \lambda_1, I), \quad (6)$$

$$X_{n-1}^* = F(X_{n-2}^*, \lambda_{n-1}, I). \quad (7)$$

As is indicated in the above formulas, the output of the previous stage is used as the input for the next stage.

Finally, it is necessary to clarify the meaning of the parameters in formula (7) as well as an important rule.  $n$  is the number of cascade single scale models.  $\lambda_i$  is the number of superpixel blocks at the  $i$ -th scale. As we defined before, the scale here is not the size but the number of superpixel blocks. And keep  $\lambda_i > \lambda_{i-1}$  in mind.

The performance of the multiscale superpixel model exceeds that of a single scale in the experiments of ADE20K below, which proves the effectiveness of the multiscale model and further demonstrates the superiority of superpixel in guiding the message passing of high-level features.

## Network Architecture

In this paper, We use DeeplabV3+ (Chen et al. 2018) as the baseline of our experiments. The information passing of superpixel is carried out after the depthwise separable convolution layers of DeeplabV3+, which is before the classifier. The overall structure is shown in Fig. 4, where the superpixel model we design is plug-and-play and can be easily embedded in the network for end-to-end training and testing. Besides, as is described above, our method is simple to implement but the performances in the next section show its effectiveness and generalizability thanks to the sharp edge of superpixel blocks. Finally, since no additional convolution structures are introduced, the parameters of the network model are not increased.

## Experiment

To evaluate the proposed method, we conduct extensive experiments on three outstanding neural networks and four widely used sense parsing datasets. In this section, we first introduce implementation details followed by the comparisons with our baselines. Then we perform ablation studies to verify the superiority of the proposed method on the ADE20K dataset. Besides, we compare our method with DenseCRF and SegFix both on mIoU and F-score. Finally, we report our results on the Cityscapes dataset, PASCAL VOC dataset, and PASCAL Context dataset.

### Implementation Details

All our experiments are based on MMSegmentation (Contributors 2020). We use ResNet (He et al. 2016) (pretrained on ImageNet (Russakovsky et al. 2015)) as our backbone. The output stride of the backbone is set to 8. Following prior works (Chen et al. 2017b; Zhao et al. 2017), we employ a poly learning rate strategy where the initial learning rate is multiplied by  $(1 - \text{iter}/\text{totaliter})^{0.9}$  after each iteration, which is set to 80000 as the maximum number of iterations in all experiments. The initial learning rate is set to be 0.01 for all datasets. Momentum and weight decay coefficients are set to 0.9 and 0.0005, respectively. For data augmentation, we apply the common scale (0.5 to 2.0), cropping and flipping of the image to augment the training data. The synchronized batch normalization is adopted in all experiments, together with the multi-grid (Chen et al. 2017b).

Input size for ADE20K dataset is set to  $512 \times 512$ , while input size for Cityscapes dataset is set to  $769 \times 769$ . For PASCAL VOC and PASCAL Context, the input size is set to  $512 \times 512$  and  $480 \times 480$  respectively. The batch size on ADE20K, PASCAL VOC, and PASCAL Context is set to 16 and Cityscapes is set to 8 due to the limited calculation resource. We train 40K iterations on PASCAL VOC and 80K iterations on ADE20K, Cityscapes, PASCAL Context.

### Comparisons with Baselines on ADE20K

In order to prove the effectiveness of the proposed method, we compare with DeeplabV3+ (Chen et al. 2018) on the validation set of ADE20K. We report the mIoU of each network structure on different backbones in Tab. 5. It is shown that the network structures equipped with our superpixel-based method have achieved excellent performances compared with the original ones. More specifically, our single scale method based on DeeplabV3+ with backbone ResNet101 achieves 45.47% in mIoU, and outperforms the original one by 0.56%. The multiscale solution with ResNet-50 and ResNet-101 achieves 43.93% and 45.81% respectively in mIoU, and outperforms the single scale solution by 0.61% and 0.34% respectively. A multiscale manner can compensate for the omission of information caused by a single scale, and this fashion can simultaneously capture longer and more effective dependency as well. Some visualization results compared with baseline are shown in Fig. 5.



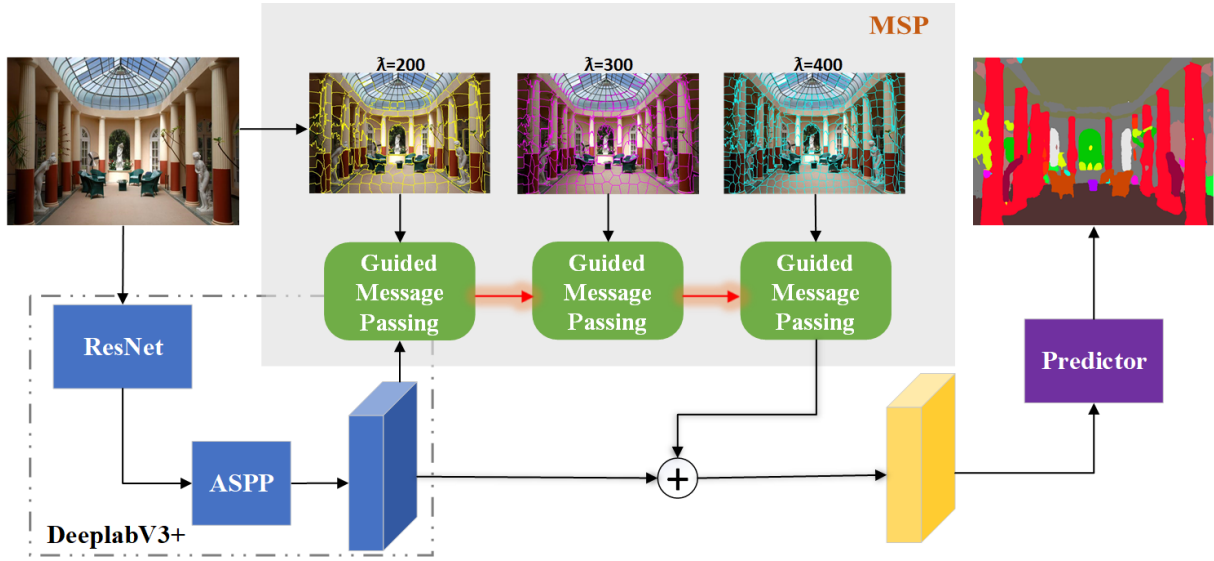


Figure 4: An overview of our network based on DeeplabV3+.

Method	Backbone	SSP	MSP	mIoU(%)
DeeplabV3+	ResNet50			42.91
DeeplabV3+	ResNet50	✓		43.32
DeeplabV3+	ResNet50		✓	<b>43.93</b>
DeeplabV3+	ResNet101			44.91
DeeplabV3+	ResNet101	✓		45.47
DeeplabV3+	ResNet101		✓	<b>45.81</b>

Table 1: **SSP**: Single scale superpixel Module. **MSP**: Multi-scale superpixel Module. The multiscale method works better than the single scale approach, and shows great potential. We believe that the reason is that the multiscale method contains more useful information and larger spatial dependencies. In the single scale model,  $\lambda$  is set to 200, while in the multiscale model,  $\lambda$  is set to 200, 300, and 400 respectively.

### Ablation Studies on ADE20K

The ADE20K dataset is one of the most challenging benchmarks, which contains 150 classes and a variety of scenes with 1,038 image-level labels. We follow the official protocol to split the whole dataset. Like most previous works, we use the mean of Intersection over Union (mIoU) for evaluation. Single scale images are adopted as input for testing by default if not specified. For ablation experiments, we adopt ResNet-50 and ResNet-101 as our backbones.

**Different Superpixel Algorithms** To explore how different algorithms affect the segmentation performance, we have conducted an ablation study on three different kinds of algorithms. They are density-based Quick Shift (QS) (Vedaldi and Soatto 2008), clustering-based SLIC (Achanta et al. 2012), and CNN-based SSN (Jampani et al. 2018). We adopt single scale superpixel guided message passing method and set  $\lambda$  to 200 for all the experiments. DeeplabV3+ with backbone ResNet-50 is served as our baseline. The result is reported in

QS	SLIC	SSN	mIoU(%)
			42.91
✓			43.19
	✓		43.32
		✓	43.47

Table 2: Comparisons with different superpixel algorithms.

Tab. 2. Though SSN achieves the best performance, it needs extra training time. On the other hand, SLIC, as an unsupervised clustering-based superpixel method, also performs well. Thus, we use SLIC for a fast implementation.

**Different Numbers of Superpixel and Scales** In order to explore the internal relationship between segmentation performance and superpixel property, we have conducted abundant experiments on different numbers of scales and combinations of different superpixel numbers. As the two ablation studies are deeply correlative, we integrate them together for better comparisons. The results are reported in Tab. 3. As is indicated in this table, it seems that multiscale  $\lambda$  set to 200, 300, and 400 performs the best. Obviously, it achieves a beautiful balance between large dependency and superpixel quality.

### Comparisons with DenseCRF and SegFix

The sharp edges of the superpixel blocks allow the adjacent boundary features from different sides to receive the information from corresponding inside superpixel blocks when the message is passing. In other words, superpixel greatly enhances the separability of the boundary because of its own sharp boundary. In this section, we compare our method with some edge optimization algorithms. Here we mainly choose DenseCRF (Krähenbühl and Koltun 2012) and SegFix (Yuan et al. 2020). We keep the same setting of DenseCRF with Deeplab (Chen et al. 2014) and fine-tune its parameters for

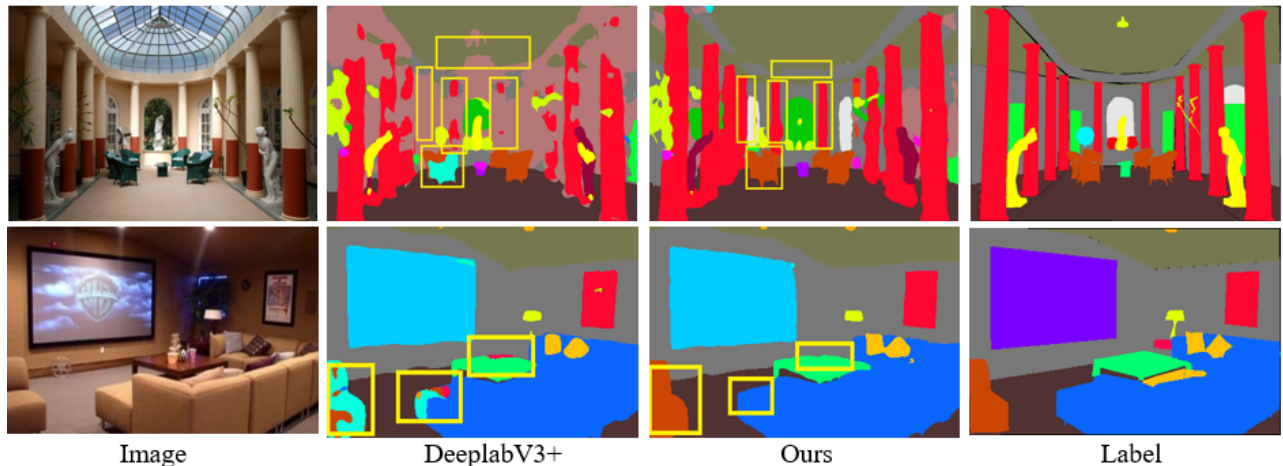


Figure 5: Qualitative comparisons between our method and baseline on ADE20K validation set. It can be seen that our method can better segment objects with consistent textures or colors, such as the pillars and sofas in the first row. Moreover, it can also smooth the edges better, such as the sofa and coffee table in the second row. These all result from the local similarity of the low-level features of superpixels and the sharp edges between pixel blocks.

Scale	100	200	300	400	500	mIoU(%)
0						42.91
1	✓					42.84
		✓				43.32
			✓			43.39
				✓		43.52
					✓	42.59
2	✓	✓				43.12
		✓	✓			43.48
			✓	✓		43.74
3	✓	✓	✓			43.36
		✓	✓	✓		<b>43.93</b>
4	✓	✓	✓	✓		43.56

Table 3: Comparisons on the ADE20K val set with DeepLabV3+ (ResNet50) as baseline. Since the damage is up to **0.32%** while  $\lambda$  is set to 500, we no longer take  $\lambda = 500$  into account for multiscale.

better performance. As for SegFix, we follow the training strategy in (Yuan et al. 2020), and train SegFix 80000 iterations on the ADE20K training set. Then for fair comparisons, the two post-processing algorithms are applied to refine the prediction of DeeplabV3+ on the ADE20K validation set, in which our method is embedded. In addition, we also superimpose the two algorithms and our method to further improve the segmentation on the ADE20K validation set.

The result is reported in Tab. 4. As is indicated in the table, our solution reaches the best performance on both mIoU and F-score among all the algorithms. And it can be seen that DenseCRF has brought a limited gain in mIoU and has a weak effect on the improvement of the object boundaries. Moreover, our experiments show that our method is also complementary with the SegFix.

DenseCRF	SegFix	MSP	mIoU(%)	F-score
			44.91	20.23
✓			45.43	21.86
	✓		45.62	22.19
		✓	<b>46.61</b>	22.34
✓		✓	46.62	23.26
	✓	✓	<b>47.05</b>	24.01
✓	✓	✓	47.00	24.65

Table 4: Comparisons with DenseCRF and SegFix on ADE20K validation set. We take Deeplabv3+ (ResNet101) as the baseline. The post-processing method of DenseCRF and SegFix brings slightly lower gains than our multiscale superpixel solution. When the multiscale superpixel method is combined with SegFix, the mIoU on the ADE20K validation set reaches **47.05%**.

### Generalizability on Other Methods

To verify the effectiveness and generalizability of our proposed MSP, we have conducted extensive experiments based on two different baselines, namely PSPNet (Zhao et al. 2017) and DeeplabV3 (Chen et al. 2017b) on the validation set of ADE20K. The results are reported in Tab. 5 and Tab. 6. As is indicated, our method can bring a relatively large gain to the two networks. Specifically, our method based on PSPNet with backbone ResNet-101 achieves 44.41% in mIoU, and outperforms the original one by 0.84%. Our method based on DeeplabV3 with backbone ResNet-101 achieves 44.89% in mIoU, and outperforms the original one by 0.81%.

### Generalizability on Other Datasets

To further verify the effectiveness and generalizability of our proposed MSP, we have conducted extensive experiments on three another datasets, namely Cityscapes, PASCAL VOC, and PASCAL Context.

Method	Backbone	MSP	mIoU(%)
PSPNet	ResNet50		41.23
PSPNet	ResNet50	✓	<b>41.99</b>
PSPNet	ResNet101		43.57
PSPNet	ResNet101	✓	<b>44.41</b>

Table 5: Comparisons with PSPNet on ADE20K dataset.

Method	Backbone	MSP	mIoU(%)
DeeplabV3	ResNet50		42.42
DeeplabV3	ResNet50	✓	<b>43.16</b>
DeeplabV3	ResNet101		44.08
DeeplabV3	ResNet101	✓	<b>44.89</b>

Table 6: Comparisons with DeeplabV3 on ADE20K dataset.

**Cityscapes** Cityscapes is another popular dataset for scene parsing, which contains totally 19 classes. It consists of 5K high-quality pixel-annotated images collected from 50 cities in different seasons, all of which are with  $1024 \times 2048$  pixels. In this data set, the training set contains 2975 finely annotated pictures, the validation set contains 500 pictures, and the test set contains 1525 pictures.

Method	Backbone	MSP	mIoU(%)
DeeplabV3+	ResNet50		79.24
DeeplabV3+	ResNet50	✓	<b>79.79</b>
DeeplabV3+	ResNet101		79.93
DeeplabV3+	ResNet101	✓	<b>80.49</b>

Table 7: Comparisons on the Cityscapes validation set with baseline DeeplabV3+. All experiments in the table adopt single scale image as input for network. And since the raw image is  $1024 \times 2048$ , in order to maintain the quality of the superpixel block, we adjust  $\lambda$  to 100 and 200 naturally while in MSP mode. **MSP** : Multiscale Superpixel Module.

For the sake of a fair comparison, we adopt ResNet-50 and ResNet-101 as our backbones respectively. Taking DeeplabV3+ as the baseline, we use 2975 finely annotated images in the Cityscapes dataset for training, and 500 images in the validation set and 1525 images in test set for evaluation with single scale input. The results can be found in Tab. 7 and Tab. 8 respectively. It is obvious that the proposed approach outperforms DeeplabV3+ in both val and test sets. More specifically, We achieve **80.49%** and **80.14%** in mIoU with ResNet-101 as backbone on the validation and test set, outperforming the baselines by **0.56%** and **0.92%**, which further demonstrates the effectiveness of our method.

**PASCAL VOC** Experiments on the PASCAL VOC dataset are conducted based on DeeplabV3+ with ResNet-101 and ResNet-50 as the backbone, respectively. Quantitative results of PASCAL VOC are shown in Tab. 9. Our method has outperformed baseline remarkably and brought **0.83 %** (ResNet-50) and **0.87%** (ResNet-101) gains in mIoU. It seems that our method is generally beneficial.

**PASCAL Context** We have conducted experiments on the PASCAL Context dataset as well. In the experiments, we set

Method	Backbone	MSP	mIoU(%)
DeeplabV3+	ResNet50		78.23
DeeplabV3+	ResNet50	✓	<b>78.98</b>
DeeplabV3+	ResNet101		79.22
DeeplabV3+	ResNet101	✓	<b>80.14</b>

Table 8: Comparisons on the Cityscapes test set with baseline DeeplabV3+. We keep the same setting as cityscapes val set.

Method	Backbone	MSP	mIoU(%)
DeeplabV3+	ResNet50		76.81
DeeplabV3+	ResNet50	✓	<b>77.64</b>
DeeplabV3+	ResNet101		78.62
DeeplabV3+	ResNet101	✓	<b>79.49</b>

Table 9: Comparisons on the PASCAL VOC set with baseline DeeplabV3+. We set  $\lambda$  to 100 and 200 while in MSP mode. Single scale images are also adopted as input for network in all experiments.

$\lambda$  to 100 and 200 while in MSP mode following PASCAL VOC. When it comes to evaluation, we adopt single scale images as input for network. Comparisons with baseline are shown in Tab. 10. As is indicated in the table, our approach achieves **48.11 %** in mIoU and outperforms DeeplabV3+ by **0.84 %** with ResNet-101 as the backbone.

Method	Backbone	MSP	mIoU(%)
DeeplabV3+	ResNet101		47.27
DeeplabV3+	ResNet101	✓	<b>48.11</b>

Table 10: Comparisons on the PASCAL Context set.

## Conclusion

In this paper, we propose a simple but effective message passing method for the use of superpixel that contains sharp boundary in semantic segmentation, which has brought general gains to our baselines on ADE20K, Cityscapes, PASCAL VOC, and PASCAL Context datasets. However, we just make a small step of exploration in how to use superpixel appropriately. In our opinion, mature superpixel algorithms are of great help to semantic segmentation and even various aspects of computer vision tasks, such as instance segmentation, object detection, saliency estimation, and so on. We will also attempt to dive deep into the follow-up research.

## References

- Achanta, R.; Shaji, A.; Smith, K.; Lucchi, A.; Fua, P.; and Süsstrunk, S. 2012. SLIC superpixels compared to state-of-the-art superpixel methods. *IEEE transactions on pattern analysis and machine intelligence*, 34(11): 2274–2282.
- Acuna, D.; Kar, A.; and Fidler, S. 2019. Devil is in the edges: Learning semantic boundaries from noisy annotations. In *Proceedings of the IEEE/CVF Conference on Computer Vision and Pattern Recognition*, 11075–11083.
- Bertasius, G.; Shi, J.; and Torresani, L. 2016. Semantic segmentation with boundary neural fields. In *Proceedings of the IEEE conference on computer vision and pattern recognition*, 3602–3610.

- Chen, L.-C.; Papandreou, G.; Kokkinos, I.; Murphy, K.; and Yuille, A. L. 2014. Semantic image segmentation with deep convolutional nets and fully connected crfs. *arXiv preprint arXiv:1412.7062*.
- Chen, L.-C.; Papandreou, G.; Kokkinos, I.; Murphy, K.; and Yuille, A. L. 2017a. Deeplab: Semantic image segmentation with deep convolutional nets, atrous convolution, and fully connected crfs. *IEEE transactions on pattern analysis and machine intelligence*, 40(4): 834–848.
- Chen, L.-C.; Papandreou, G.; Schroff, F.; and Adam, H. 2017b. Rethinking atrous convolution for semantic image segmentation. *arXiv preprint arXiv:1706.05587*.
- Chen, L.-C.; Zhu, Y.; Papandreou, G.; Schroff, F.; and Adam, H. 2018. Encoder-decoder with atrous separable convolution for semantic image segmentation. In *Proceedings of the European conference on computer vision (ECCV)*, 801–818.
- Chen, X.; Williams, B. M.; Vallabhaneni, S. R.; Czanner, G.; Williams, R.; and Zheng, Y. 2019. Learning active contour models for medical image segmentation. In *Proceedings of the IEEE/CVF Conference on Computer Vision and Pattern Recognition*, 11632–11640.
- Contributors, M. 2020. MMSegmentation: OpenMMLab Semantic Segmentation Toolbox and Benchmark. <https://github.com/open-mmlab/mms Segmentation>.
- Cordts, M.; Omran, M.; Ramos, S.; Rehfeld, T.; Enzweiler, M.; Benenson, R.; Franke, U.; Roth, S.; and Schiele, B. 2016. The Cityscapes Dataset for Semantic Urban Scene Understanding. In *Proc. of the IEEE Conference on Computer Vision and Pattern Recognition (CVPR)*.
- Ding, H.; Jiang, X.; Liu, A. Q.; Thalmann, N. M.; and Wang, G. 2019. Boundary-aware feature propagation for scene segmentation. In *Proceedings of the IEEE/CVF International Conference on Computer Vision*, 6819–6829.
- Everingham, M.; Eslami, S. A.; Van Gool, L.; Williams, C. K.; Winn, J.; and Zisserman, A. 2015. The pascal visual object classes challenge: A retrospective. *International journal of computer vision*, 111(1): 98–136.
- Fu, J.; Liu, J.; Tian, H.; Li, Y.; Bao, Y.; Fang, Z.; and Lu, H. 2019. Dual attention network for scene segmentation. In *Proceedings of the IEEE/CVF Conference on Computer Vision and Pattern Recognition*, 3146–3154.
- Gadde, R.; Jampani, V.; Kiefel, M.; Kappler, D.; and Gehler, P. V. 2016. Superpixel convolutional networks using bilateral inceptions. In *European conference on computer vision*, 597–613. Springer.
- Gould, S.; Rodgers, J.; Cohen, D.; Elidan, G.; and Koller, D. 2008. Multi-class segmentation with relative location prior. *International Journal of Computer Vision*, 80(3): 300–316.
- He, K.; Zhang, X.; Ren, S.; and Sun, J. 2016. Deep Residual Learning for Image Recognition. In *2016 IEEE Conference on Computer Vision and Pattern Recognition (CVPR)*, 770–778.
- He, S.; Lau, R. W.; Liu, W.; Huang, Z.; and Yang, Q. 2015. Supercnn: A superpixelwise convolutional neural network for salient object detection. *International journal of computer vision*, 115(3): 330–344.
- Huang, Z.; Wang, X.; Huang, L.; Huang, C.; Wei, Y.; and Liu, W. 2019. Ccnet: Criss-cross attention for semantic segmentation. In *Proceedings of the IEEE/CVF International Conference on Computer Vision*, 603–612.
- Jampani, V.; Sun, D.; Liu, M.-Y.; Yang, M.-H.; and Kautz, J. 2018. Superpixel sampling networks. In *Proceedings of the European Conference on Computer Vision (ECCV)*, 352–368.
- Ke, T.-W.; Hwang, J.-J.; Liu, Z.; and Yu, S. X. 2018. Adaptive affinity fields for semantic segmentation. In *Proceedings of the European Conference on Computer Vision (ECCV)*, 587–602.
- Krähenbühl, P.; and Koltun, V. 2012. Efficient inference in fully connected crfs with gaussian edge potentials. *arXiv preprint arXiv:1210.5644*.
- Krizhevsky, A.; Sutskever, I.; and Hinton, G. E. 2012. Imagenet classification with deep convolutional neural networks. *Advances in neural information processing systems*, 25: 1097–1105.
- Li, X.; Zhong, Z.; Wu, J.; Yang, Y.; Lin, Z.; and Liu, H. 2019. Expectation-Maximization Attention Networks for Semantic Segmentation. In *International Conference on Computer Vision*.
- Lin, G.; Milan, A.; Shen, C.; and Reid, I. 2017a. Refinenet: Multi-path refinement networks for high-resolution semantic segmentation. In *Proceedings of the IEEE conference on computer vision and pattern recognition*, 1925–1934.
- Lin, T.-Y.; Dollár, P.; Girshick, R.; He, K.; Hariharan, B.; and Belongie, S. 2017b. Feature pyramid networks for object detection. In *Proceedings of the IEEE conference on computer vision and pattern recognition*, 2117–2125.
- Long, J.; Shelhamer, E.; and Darrell, T. 2015. Fully convolutional networks for semantic segmentation. In *Proceedings of the IEEE conference on computer vision and pattern recognition*, 3431–3440.
- Mottaghi, R.; Chen, X.; Liu, X.; Cho, N.-G.; Lee, S.-W.; Fidler, S.; Urtasun, R.; and Yuille, A. 2014. The role of context for object detection and semantic segmentation in the wild. In *Proceedings of the IEEE conference on computer vision and pattern recognition*, 891–898.
- Peng, C.; Zhang, X.; Yu, G.; Luo, G.; and Sun, J. 2017. Large kernel matters—improve semantic segmentation by global convolutional network. In *Proceedings of the IEEE conference on computer vision and pattern recognition*, 4353–4361.
- Perazzi, F.; Krähenbühl, P.; Pritch, Y.; and Hornung, A. 2012. Saliency filters: Contrast based filtering for salient region detection. In *2012 IEEE conference on computer vision and pattern recognition*, 733–740. IEEE.
- Ren, X.; and Malik, J. 2003. Learning a classification model for segmentation. In *Computer Vision, IEEE International Conference on*, volume 2, 10–10. IEEE Computer Society.
- Russakovsky, O.; Deng, J.; Su, H.; Krause, J.; Satheesh, S.; Ma, S.; Huang, Z.; Karpathy, A.; Khosla, A.; Bernstein, M.; et al. 2015. Imagenet large scale visual recognition challenge. *International journal of computer vision*, 115(3): 211–252.
- Sharma, A.; Tuzel, O.; and Liu, M.-Y. 2014. Recursive Context Propagation Network for Semantic Scene Labeling. In *NIPS*, volume 1, 2.
- Shu, G.; Dehghan, A.; and Shah, M. 2013. Improving an object detector and extracting regions using superpixels. In *Proceedings of the IEEE Conference on Computer Vision and Pattern Recognition*, 3721–3727.
- Simonyan, K.; and Zisserman, A. 2014. Very deep convolutional networks for large-scale image recognition. *arXiv preprint arXiv:1409.1556*.
- Stutz, D.; Hermans, A.; and Leibe, B. 2018. Superpixels: An evaluation of the state-of-the-art. *Computer Vision and Image Understanding*, 166: 1–27.
- Szegedy, C.; Liu, W.; Jia, Y.; Sermanet, P.; Reed, S.; Anguelov, D.; Erhan, D.; Vanhoucke, V.; and Rabinovich, A. 2015. Going deeper with convolutions. In *Proceedings of the IEEE conference on computer vision and pattern recognition*, 1–9.



- Takikawa, T.; Acuna, D.; Jampani, V.; and Fidler, S. 2019. Gated-scnn: Gated shape cnns for semantic segmentation. In *Proceedings of the IEEE/CVF International Conference on Computer Vision*, 5229–5238.
- Van den Bergh, M.; Boix, X.; Roig, G.; de Capitani, B.; and Van Gool, L. 2012. Seeds: Superpixels extracted via energy-driven sampling. In *European conference on computer vision*, 13–26. Springer.
- Vedaldi, A.; and Soatto, S. 2008. Quick shift and kernel methods for mode seeking. In *European conference on computer vision*, 705–718. Springer.
- Wang, X.; Girshick, R.; Gupta, A.; and He, K. 2018a. Non-local neural networks. In *Proceedings of the IEEE conference on computer vision and pattern recognition*, 7794–7803.
- Wang, X.; Girshick, R.; Gupta, A.; and He, K. 2018b. Non-local neural networks. In *Proceedings of the IEEE conference on computer vision and pattern recognition*, 7794–7803.
- Weikersdorfer, D.; Schick, A.; and Cremers, D. 2013. Depth-adaptive supervoxels for RGB-D video segmentation. In *2013 IEEE International Conference on Image Processing*, 2708–2712. IEEE.
- Yan, J.; Yu, Y.; Zhu, X.; Lei, Z.; and Li, S. Z. 2015. Object detection by labeling superpixels. In *Proceedings of the IEEE Conference on Computer Vision and Pattern Recognition*, 5107–5116.
- Yang, C.; Zhang, L.; Lu, H.; Ruan, X.; and Yang, M.-H. 2013. Saliency detection via graph-based manifold ranking. In *Proceedings of the IEEE conference on computer vision and pattern recognition*, 3166–3173.
- Yuan, Y.; Xie, J.; Chen, X.; and Wang, J. 2020. Segfix: Model-agnostic boundary refinement for segmentation. In *European Conference on Computer Vision*, 489–506. Springer.
- Zhao, H.; Shi, J.; Qi, X.; Wang, X.; and Jia, J. 2017. Pyramid scene parsing network. In *Proceedings of the IEEE conference on computer vision and pattern recognition*, 2881–2890.
- Zheng, S.; Jayasumana, S.; Romera-Paredes, B.; Vineet, V.; Su, Z.; Du, D.; Huang, C.; and Torr, P. H. 2015. Conditional random fields as recurrent neural networks. In *Proceedings of the IEEE international conference on computer vision*, 1529–1537.
- Zhou, B.; Zhao, H.; Puig, X.; Fidler, S.; Barriuso, A.; and Torralba, A. 2017. Scene Parsing through ADE20K Dataset. In *Proceedings of the IEEE Conference on Computer Vision and Pattern Recognition*.
- Zhu, W.; Liang, S.; Wei, Y.; and Sun, J. 2014. Saliency optimization from robust background detection. In *Proceedings of the IEEE conference on computer vision and pattern recognition*, 2814–2821.